FTIR Analysis of Alkali Activated Slag and Fly Ash Using Deconvolution Techniques

by

Sateesh Babu Madavarapu

A Thesis Presented in Partial Fulfillment
of the Requirement for the Degree
Master of Science

Approved July 2014 by the
Graduate Supervisory Committee:

Narayanan Neithalath, Chair
Subramaniam Rajan
Robert Marzke

ARIZONA STATE UNIVERSITY

August 2014

ABSTRACT

The studies on aluminosilicate materials to replace traditional construction materials such as ordinary Portland cement(OPC) to reduce the effects caused has been an important research area for the past decades. Many properties like strength have already been studied and the primary focus is to learn about the reaction mechanism and the effect of the parameters on the formed products. The aim of this research was to explore the structural changes and reaction product analysis of geopolymers (Slag & Fly Ash) using Fourier transform infrared spectroscopy (FTIR) and deconvolution techniques. Spectroscopic techniques give valuable information at a molecular level but not all methods are economic and simple. To understand the mechanisms of alkali activated aluminosilicate materials, attenuated total reflectance (ATR) FTIR has been used where the effect of the parameters on the reaction products have been analyzed. To analyze complex systems like geopolymers using FTIR, deconvolution techniques help to obtain the properties of a particular peak attributed to a certain molecular vibration.

Time and temperature dependent analysis were done on slag pastes to understand the polymerization of reactive silica in the system with time and temperature variance. For time dependent analysis slag has been activated with sodium and potassium silicates using two different 'n'values and three different silica modulus [M_s- (SiO_2 /M_2O)] values. The temperature dependent analysis was done by curing the samples at 60°C and 80°C. Similarly fly ash has been studied by activating with alkali hydroxides and alkali silicates. Under the same curing conditions the fly ash samples were evaluated to analyze the effects of added silicates for alkali activation.

The peak shifts in the FTIR explains the changes in the structural nature of the matrix and can be identified using the deconvolution technique. A strong correlation is found between the concentrations of silicate monomer in the activating position of

the main Si-O-T (where T is Al/Si) stretching band in the FTIR spectrum, which gives an indication of the relative changes in the Si/Al ratio. Also, the effect of the cation and silicate concentration in the activating solution has been discussed using the Fourier self deconvolution technique.

ACKNOWLEDGEMENTS

I am grateful to many people who helped me in one way or other for completing my Masters thesis.

First of all I thank my parents, brothers and sister-in-law for being there for me throughout and believing in my ability to pursue my Masters degree.

I would like to express my deep and sincere gratitude to my advisor Dr. Narayanan Neithalath for his encouragement, inspiration and insightful discussions. He is always friendly and approachable even for unscheduled appointments.

I would also like to thank my thesis committee members, Dr. Subramaniam Rajan and Dr. Robert Marzke for consenting to examine my thesis.

My special thanks to Akash for his valuable comments and help throughout. I also thank my lab mates Sumanta, Kirk, Aashay, Matt, Pu for all their help and valuable inside throughout my research.

I am thankful for my roommates for being my family away from home and supporting me in every situation and special thanks to Kishore for helping me in preparing this report. I am also thankful to my friends at Arizona State University for helping me in every way during my stay at ASU.

Finally, I would like to give acknowledgement to Arizona State University School of Sustainable Engineering and Built Environment for permitting me to use their laboratory facilities which allowed me to pursue my M.S in Civil Engineering.

TABLE OF CONTENTS

CHAPTER Page

LIST OF TABLES

LIST OF FIGURES

Figure Page

Chapter 1

INTRODUCTION

Urbanization lead to an increased demand for growth of construction industry enhancing the cement production causing a growth in the release of greenhouse gases which affect the environment. Understanding the benefits of using alkali activated geopolymers as the primary binding material in place of traditional cement (OPC) has been extensive for the past years. Due to their capability to form durable products, their application in to the industry is gaining focus [1], [2], [3]. These geopolymers include slag, fly ash, metakaolin etc. Activating these materials with an alkaline medium provide a strong durable material which is sustainable compared to the OPC products. Although these materials provide enormous strength results, it is important to understand the reaction mechanism in a better scale so that the influence of the parameters used to prepare these materials can be understood. Various mechanisms and techniques can be used but spectroscopic methods explain the product formation in a scientific perspective. Fourier Transform Infrared Spectroscopic technique has been used to study these materials. Although there are other effective spectroscopic methods to analyze, FTIR technique is more economic and robust to analyze many different samples [4], [5], [6]. The significance of various bonds in a material matrix can be understood from its FTIR spectra. The spectrum of a material is a unique result as no two materials can be completely same in composition or molecular structure.

The spectra obtained from a FTIR instrument is an integrated result with the combination of many different bands. In complex systems like alkali activated geopolymers, these combinations are higher in number. To analyze different individual bonds using the FTIR spectra, deconvolution techniques can be used which provide the de-

tails of the intrinsic overlapping bands that determine significance of various bonds. Fourier Self deconvolution technique has been used in many of the studies to deconvolute the obtained infrared spectra. The parameters used for this technique also govern the results but it is important to use the feasible values.

The materials used in this study are slag and fly ash which are activated using different alkaline media[7], [8], [9], [10]. The focus is on the influence of the binding materials, properties of the activators. Study on alkali activated slag also focuses on the effect of curing time and temperature. The influence of all these factors provides more information for the usage of these systems on larger scale.

1.1 Thesis Objectives

1. Evaluate and understand the effects of parameters ('n'and 'M_s'), curing time and temperature on the alkali silicate activated slag using FTIR deconvolution technique. Also, the influence of cation (Na and K) on alkali activated slag over time has been analyzed.
2. Analyze the influence of added silicate in the alkali activation of fly ash using FTIR results. The effect of cation (Na and K) and initial parameters were also evaluated for alkali activated fly ash.

1.2 Thesis Layout

Chapter 2 provides a literature review of past FTIR studies on alkali activated aluminosilicate materials. Also a review on the Fourier self deconvolution technique discussing the various parameters involved in the program.

Chapter 3 provides the experimental design, including raw material properties, chemical compositions, mixture proportions, mixing procedures and test method to assess the properties of alkali activated slag and fly ash systems.

Chapter 4 provides a detailed review of FTIR spectroscopy and its deconvolution

techniques. The parameters that influence the deconvolution are discussed such as line shape function, apodization function, half width at half maximum etc and also how these parameters were chosen has been explained.

Chapter 5 explains the effect of curing conditions i.e. time and temperature on the reaction product analysis of alkali activated slag systems. Also, the influence of the parameters ('n'and 'M_s') evaluating the effect of cation (Na and K) has been detailed.

Chapter 6 details the effect of activator concentrations on reaction products of alkali activated fly ash systems. The influence of added silicates on the results has been discussed in detail.

Chapter 7 provides a detailed conclusion of the studies carried out on the alkali activated binder systems.

Chapter 2

LITERATURE REVIEW

Construction industries use cement (OPC) as the primary binding material which increases the demand for its production as it is not a naturally available material. A huge amount of cement is produced on a daily basis consuming so much energy with the release of vast volumes of carbon di oxide in to the atmosphere[11]. The world is advancing in to an era of modern infrastructure where environmental conservation is a big concern. Research has been going on to explore the possibilities of alternative methods to the usage of cement. Some industrial by products like fly ash and slag are added to the cement mixes to attain better products. These materials also concerns the environmental conservations as they are disposed in the landfills after produced as industrial wastes. In order to overcome such problems, better usage of these materials in a productive way has been a big interest in the industry. These geopolymers are also cementitious materials which can obtain better physical and chemical characteristics like durability, strength, thermal stability without the emission of greenhouse gases and consumption of energy. The reuse of these industrial wastes is sustainable and also reduces the demand for cement production which is beneficial for the environment. When activated in an alkaline medium these aluminosilicates undergo a series of physiochemical reactions which result in a solid structured product [8]-[11],[12], [13], [14]. First the alkalinity releases the free ions and the alkali severs some silicate bonds incorporating aluminum in to the structure and then repolymerizes to form a chained network binding the individual structures together [9],[13], [14], [15], [16], [17], [18]. These geopolymer concretes exhibit comparable properties w.r.t traditional concretes without consumption of energy and emission of greenhouse gases in to the

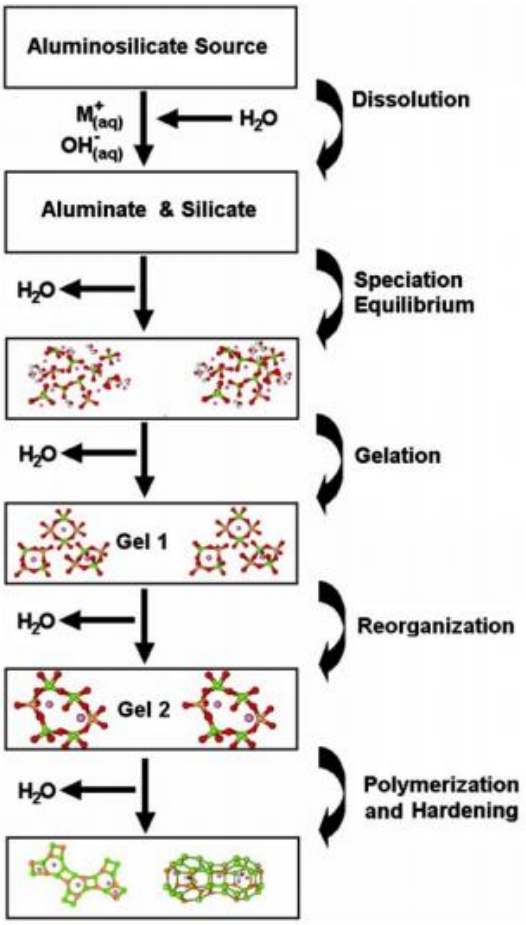

Figure 2.1: Conceptual Model for Geopolymerization (Source- Duxson et al).

environment. But the strength in the cement concretes come from the pozzolanic reaction whereas in the geopolymers the polymerization of silica and alumina in the matrix creates their strength. Although the types of products formed are not the same in all these materials. Ground granulated slag is rich in calcium hence the product formed has a high calcium content. Whereas fly ash is low in calcium content and the product formed is mainly due to the polymerized chains of silica and alumina [19], [20], [21], [22].

It is important to understand the importance of parameters that dictates the

product formation. Understanding the series of reactions at a molecular level helps to optimize the properties of these parameters and can attain reaction products in a required manner.

2.1 Fourier Transform Infrared Spectroscopy

Fourier Transform Infrared spectroscopy technique is being used extensively to perform reaction product analysis on cementitious materials. Spectroscopic techniques provide molecular fingerprints of materials as every compound exhibit different types of vibrations. Attenuated Total Reflectance (ATR) FTIR is a reliable technique to analyze powder samples and has been used for this study. The peaks arising at different wavenumbers with different intensities explain the type of bond formations and vibrations in the material matrix. This helps to identify the different compositions in a material. For alkali activated aluminosilicates the peaks determining the silicate region are concentrated as the structure is defined by these chains. The analysis can be done to perform various studies like the changes occurring w.r.t time, temperature, mix proportions, curing conditions etc. The position of the Si-O-T peak (where T is Al or Si) is observed from the FTIR spectra of these samples. The range of Si-O-T peak for geopolymers is from 900- 1200 cm^{-1}. The position of peak varies due to factors like time, mix proportion etc. According to geopolymers theory an aluminum gel is formed at the beginning which later on forms a gel with more silicates in the structure polymerizing to form a solid product. When analyzing with time, the peak values of the Si-O-T peak can change due to physiochemical reactions. The decrease in wavenumber indicates lower force constant which means lower bond energy or strength. This provides us with information about the lengthening or changes in bond angles. Hence the changes happening in the aluminosilicate structures after the addition of alkali activators can be analyzed from the FTIR spectra of the reaction

products. The obtained FTIR spectrum of a material is an integrated curve mapping all the peaks determining various vibrations. The peaks with higher intensities and ranges can overlap smaller adjacent bonds and form the integrated peak. These smaller peaks can be of valuable significance for analyzing the material. Mathematical techniques can be used to deconvolute these intrinsic overlapping bands from the spectrum. Fourier self deconvolution (FSD) is a technique first applied by Kauppinen and others in the 1980 to deconvolute the overlapping bands in a spectrum and many has used the same technique for deconvolution of IR spectra. As the resultant spectra obtained from an FTIR instrument is a Fourier Transform of the actual spectra, the Fourier self deconvolution technique uses the inverse Fourier transform of the result and enhances the resolution to make these small intrinsic bands noticeable. Although the input parameters play a major role on the results, this technique has been proven reliable to identify the overlapping peaks in a complex spectra. For basic or pure materials the deconvolution can be done by curve fitting the actual FTIR spectra as many overlapping peaks may not be found. But for complex systems like alkali activated geopolymers, using a program like FSD is useful to analyze the intrinsic bands.

Chapter 3

MATERIALS, MIXTURE PROPORTIONS AND TEST METHODS

The purpose of this chapter is to describe the materials used and the methodology employed for the research presented in this thesis. The experimental procedures used to create the samples are also explained in detail, along with a description of the equipment utilized for the analysis.

3.1 Materials and Mixtures

The materials used as binder in this research are Class F flyash conforming to ASTM C 618 and ground granulated blast furnace slag conforming to ASTM C 989 [23].

3.1.1 Alkali Activation of Ground Granulated Blast Furnace Slag

The median particle size (d_{50}) of the used slag is 8.9 m as determined by dynamic light scattering. The calcium content in slag is low compared to OPC systems and the composition plays a vital role in the reaction mechanism [24], [20].

The activators used to activate slag are sodium silicate (waterglass) and potassium silicate liquid solutions. The parameters used to proportion the activating solutions are: M_2O to slag (binder) ratio ('n'value) and the silica modulus 'M_s'(SiO_2 to M_2O

Table 3.1: Chemical Composition and Properties of Slag (Binder).

SiO_2	Al_2O_3	Fe_2O_3	CaO	MgO	SO_3	Na_2O	K_2O	LOI	S.G	SSA
36%	10.5%	0.67%	39.8%	7.93%	2.10%	0.27%	0.80%	3.01%	2.90%	487 m^2/Kg

Table 3.2: Types of Activator Mixes and Proportions Used for Time Dependent Analysis.

Time Dependent Analysis												
Cation	Na						K					
n	0.03			0.05			0.03			0.05		
M_2	1	1.5	2	1	1.5	2	1	1.5	2	1	1.5	2

molar ratio). Here M is either Na or K based on the activator used. A n value is considered as a basic parameter which dictates the amount of alkali hydroxides present in the activator. Both sodium and potassium silicate activators have a solids content of 36% with a silica modulus (M_s) of 3.3. For both the silicates the respective hydroxides were added to attain lower 'M_s'values (1.0, 1.5 and 2.0). The 'M_s'values used in this research were 1.0, 1.5 and 2.0. Previous studies show that beneficial strength development is seen in this range of 'M_s'values [10], [16], [19], [25], [26], [27], [28], [29]. A water to powder ratio of 0.40 has been used which accounts for the water present in the activator solution and water is externally added to attain the required water to powder ratio. The activators were prepared for a given 'M_s'(which is attained by adding alkali silicates) a required n value is obtained by adding alkali hydroxides. The samples tested were placed in closed containers at all times and the samples used in temperature dependent analysis were heat cured at 60° C and 80° C in an oven with the samples sealed in a container preventing the exposure to environment [30].

3.1.2 Alkali Activation of Fly Ash

The silica and alumina content in fly ash is higher compared to slag as the amount of CaO is very less in fly ash. Figure 3.1 shows the particle size distribution of fly ash

Table 3.3: Types of Activator Mixes and Proportions Used for Temperature Dependent Analysis.

Temperature Dependent Analysis								
Temperature	80°				60°			
Cation	Na		K		Na		K	
n	0.03	0.05	0.03	0.05	0.03	0.05	0.03	0.05
M_s	1.5	1.5	1.5	1.5	1.5	1.5	1.5	1.5

Table 3.4: Chemical Composition and Properties of ClassF Fly Ash (Binder).

SiO_2	Al_2O_3	Fe_2O_3	CaO	Moisture	SO_3	Available Alkalis	LOI	S.G
59.62%	22.87%	4.53%	5.26%	0.04%	0.48%	0.27%	0.47%	2.26

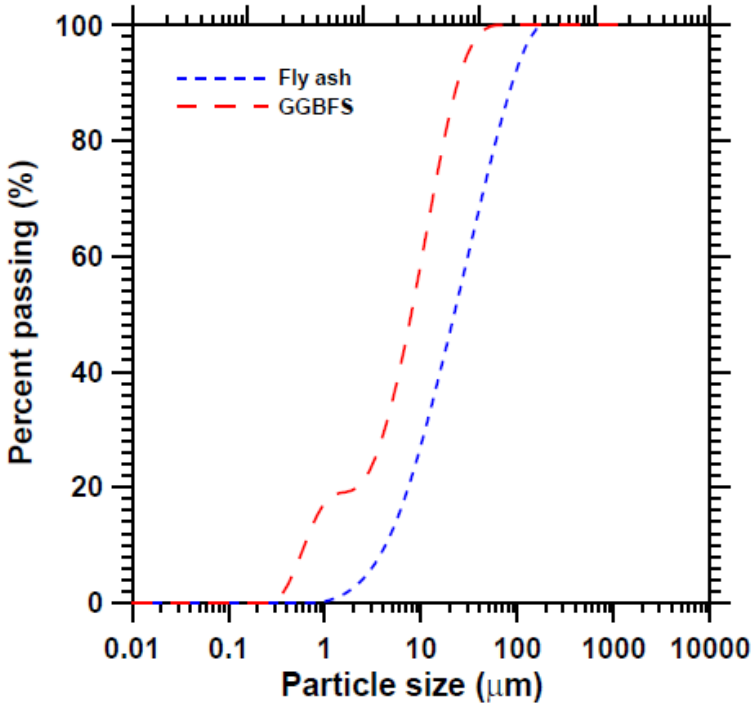

Figure 3.1: Particle size distribution of fly ash and slag (Ravikumar, Property Development, Microstructure and Performance of Alkali Activated Fly Ash and Slag Systems, 2012).

Table 3.5: Hydroxide Activators Without Any Soluble Silica Content.

Hydroxides						
Cation	Na			K		
Molarity	2	4	8	2	4	8

Table 3.6: Alkali Activators With Soluble Silica and Distinguished Based on Na/Al Ratio and M_s.

Silicate Activators						
Cation	Na					
Na/Al ratio	0.25			0.5		
M_s	0	1	2	0	1	2

and slag. The particle size analysis shows that slag is finer than fly ash with 95% of particles are finer than 30 mm compared to 60% for fly ash.

Two types of alkali activators have been used for the activation of fly ash. First one is just alkali metal hydroxides with varying molar concentrations. The required molar concentrations have been achieved by adding sodium and potassium hydroxide pellets.

The alkali silicate activators were prepared in a similar fashion of which activators for slag were prepared. But the sodium silicate activator used here is of different concentration having a solids content of 44% with a silica modulus (M_s) of 2.0. Potassium silicate activators have a solids content of 36% with a silica modulus (M_s) of 3.3. Alkali silicates are added to reach a required M_s value. Then alkali hydroxides are added to achieve a required R/Al ratio compensating with the alumina content from fly ash. All the fly ash samples were cured at 80°C for 72 hours placed and sealed in containers preventing exposure to the environment.

For silicate activators the hydroxides used to reduce the activator M_s were pre-

Table 3.7: Alkali Activators with Soluble Silica and Distinguished Based on K/Al Ratio and M_s.

Silicate Activators						
Cation	K					
K/Al ratio	0.25			0.5		
M_s	0	1	2	0	1	2

pared by dissolving in water and then are added to the required amount of alkali silicate. But for the activators without soluble silicates, the hydroxides were measured in a measuring cylinder and required amount of water is added. Same procedure was followed for both fly ash and slag activation.

3.2 Test Methods

Fourier Transform Infrared Spectroscopy experiment was done to obtain the spectra of alkali activated slag samples. Mattson Genesis Spectrometer has been used to carry out the experiments. For time dependent analysis the samples were cured at room temperature (25°C)and were tested at 6 hours, 12 hours, 1 day, 2 days, 7 days, 14 days and 28 days. The resolution used is 2 cm^{-1} and the high refractive medium is a diamond head. A 51 point Savitsky Golay - Quintic smoothing window is used to smooth the data. The absorbance v/s wavenumber plots were obtained from the instrument.

The compressive strengths were determined in accordance with ASTM C 109. The strengths were determined using 50 mm cubes and tested at intervals of 1 day, 14 days and 28 days.

Chapter 4

FTIR DECONVOLUTION TECHNIQUE AND METHODOLOGY

4.1 Fourier Transform Infrared Spectroscopy

FTIR is one of the preferred methods of infrared spectroscopy. The infrared radiation is passed through the sample where some amount of energy is absorbed and some amount is transmitted. The transmission and absorption is a unique property of a molecule in IR radiation. This makes this technique useful for many types of analysis. FTIR provides the identity, consistency and also relative quantities of different species present in the samples. The absorption or the transmittance peaks obtained from the IR spectra represent the vibrations between the atomic bonds that form the material. As the bond structure is not same in two different compounds, the IR spectra provide a unique property of a material. Also, the intensity of the peaks provides a relative variation in the quantity of different types of vibrations. FTIR spectroscopic technique has many advantages over other traditional techniques like dispersive spectroscopy. FTIR is a non-destructive technique which requires very less amount of sample. Also, due to its speed, better sensitivity, mechanical simplicity it is preferred over other spectroscopic techniques. After the light is passed through the sample the output provides information about each and every frequency coming from the source light. All these signals interfere and the result is called an interferogram. But to analyze the result it is easier to obtain the output which looks like a plot of intensity versus frequency. The Fourier transform of this output interferogram is the result that is analyzed using FTIR spectroscopy. This way molecular information at every frequency can be extracted using this technique.

4.1.1 ATR FTIR

FTIR spectroscopy can be done using various mechanisms. Attenuated total reflectance (ATR) is one of the preferred methods. The other method uses a KBr pellet where sample is covered over by this medium and analyzed for results. The sample preparation is a time taking process. ATR is a better procedure and the sample preparation is easier. The sample is placed over a reflective crystal medium where light is passed through. A portion of light is absorbed and the remaining energy travels back in to the instrument which is later converted using Fourier transform analysis and displayed. The medium is made of a material with high refractive index. Diamond is the crystal used for this study due to its robustness, inertness and durability. ATR technique can be used for both solid and liquid samples but the solid samples are to be uniformly grinded to a minute size level to obtain better results. Due to its improved spectral acquisition and reproducibility, this method is preferred over other techniques.

4.2 Fourier Self Deconvolution

Fourier Self Deconvolution is a reliable method and is widely used for spectral analysis. Given that the spectrum is comprised of overlapping bands of various silica species, it is possible to deconvolute part or all of the intrinsic species from the spectrum using line shape function. This technique reduces the instrumental resolution to a level which can convey the desired information. Initially an IR spectrum is passed through the sample which creates the noise called Interferogram. The Fourier transform of this is the obtained spectrum that we analyze. Hence the technique which involves inverse Fourier transform is feasible for the process of deconvolution. The spectral interferogram obtained is in the time domain which gets converted in

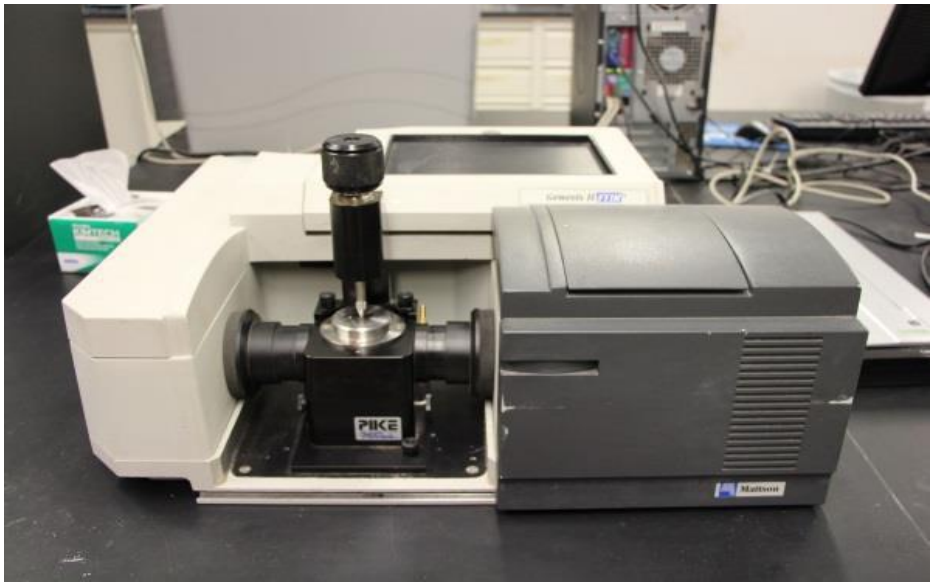

Figure 4.1: Mattson Genesis FTIR Instrument With Diamond Crystal Base.

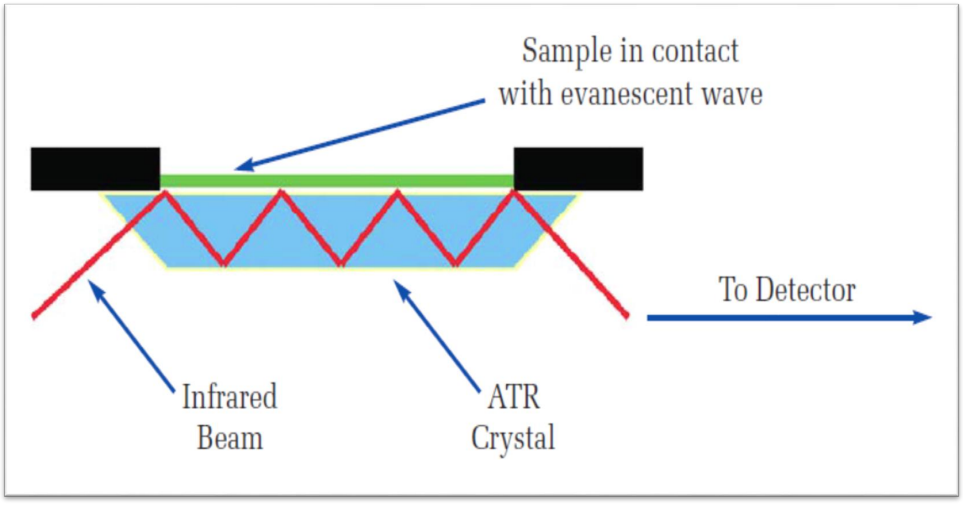

Figure 4.2: Pictorial Representation of ATR FTIR Spectroscopy.

to the frequency domain after undergoing through the Fourier transform. Here, the parameters of this spectral interferogram are altered back in the time domain to enhance the resolution in a way to obtain the desired information back in the frequency domain. Here, few parameters are assumed and few are introduced manually in to the program which can obtain results that do not manipulate the actual information from the original spectrum. An algorithm has been coded in 'MATLAB'. The algorithm has been obtained from [31], [32], [33], [34], [35].

The relationship between a spectrum and its Interferogram is given by:

$$\begin{aligned} \mathbf{E}(\bar{\nu}) &= \int_{-\infty}^{\infty} I(x)\exp(I2\pi\bar{\nu}x)dx \\ &= \mathcal{F}\{I(x)\} \end{aligned} \tag{4.1}$$

Where $\mathbf{E}(\bar{\nu})$ is the spectrum in wavenumber domain and $I(x)$ is the Interferogram and x has units in centimeters.

The FTIR spectrum obtained can be expressed as a culmination of the actual resultant spectrum and a line shape function. A line shape functions determines the shape of the curves for the spectral data.

$$\begin{aligned} \mathbf{E}(\bar{\nu}) &= \mathcal{S}(\bar{\nu}) * \mathbf{E}^{\dagger}(\bar{\nu}) \\ &= \int_{-\infty}^{\infty} \mathcal{S}(\bar{\nu}^{\dagger}) * \mathbf{E}^{\dagger}(\bar{\nu} - \bar{\nu}^{\dagger})dv^{\dagger} \end{aligned} \tag{4.2}$$

Where $\mathbf{E}^{\dagger}(\bar{\nu})$, is the actual spectrum, $\mathcal{S}(\bar{\nu})$ represents the line shape function, $*$ indicates the convolution operation

Different line shapes functions are possible but for the samples used in this work few line shape functions are used. Gaussian, Lorentzian and Voigt function.

4.2.1 Gaussian Function

The Gaussian distribution is a function determined by two parameters which are mean and its variance. The peak value represents the mean and the half width is the

variance. The probability density function for Gaussian Curve is:

$$G(x) = \frac{1}{\sigma\sqrt{2\pi}} \exp(\frac{-(x-\mu)}{2\sigma^2}) \ , \tag{4.3}$$

where x is the position, μ , is the mean or center and σ , is the half width or the variance.

4.2.2 Lorentzian Function

This distribution is also a function of mean and its variance. The probability density function for Lorentzian distribution is:

$$L(x) = \frac{1}{\pi} \frac{\sigma}{(x-\mu)^2 + \sigma^2} \ , \tag{4.4}$$

where x is the position, μ , is the mean or center and σ and σ , is the half width or the variance. Voigt function is a combination of both Gaussian and Lorentzian

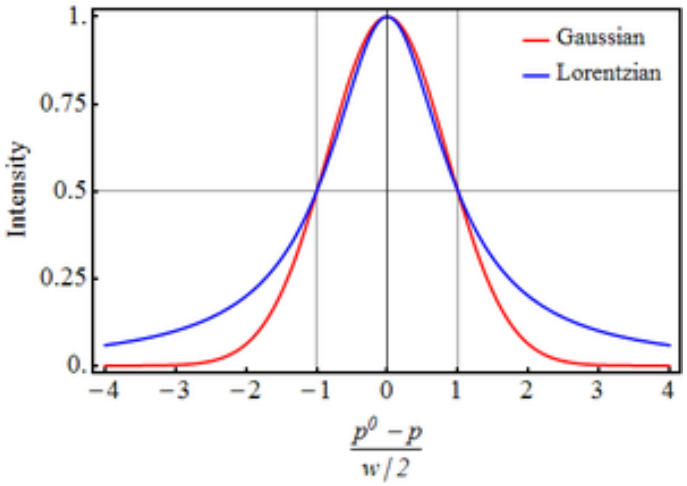

Figure 4.3: Gaussian and Lorentzian Curves.

which can be represented as the convolution of both the functions.

Form the Equation(4.2) we can observe that the obtained spectrum is a convolution of a line shape function and the actual spectrum. In order to deconvolute the

line shape function from the spectrum we take the inverse Fourier transform on both the sides. We obtain

$$\mathcal{F}^{-1}\{\mathbf{E}(\bar{\nu})\} = \mathcal{F}^{-1}\{\mathcal{S}(\bar{\nu})\}.\mathcal{F}^{-1}\{\mathbf{E}^{\dagger}(\bar{\nu})\} \tag{4.5}$$

Note: Convolution operation in frequency domain is multiplication in time domain and vice versa.

From Equation(4.1) we can say that inverse Fourier transform of $\mathbf{E}(\bar{\nu})$ is $I(x)$. Hence

$$I(x) = \mathcal{F}^{-1}\{\mathcal{S}(\bar{\nu})\}.I^{\dagger}(x) \tag{4.6}$$

All the samples here are powders and previous studies suggest that using a Gaussian shape function gives better results for powdered samples.

4.2.3 Truncation

The data obtained from the inverse Fourier transform of E() will be in time domain and is periodic with an infinite range. Window or apodization functions are used to truncate this data to a specific range. From Equation(4.6) we get $I^{\dagger}(x)$ as,

$$I^{\dagger}(x) = \frac{1}{\mathcal{F}^{-1}\{\mathcal{S}(\bar{\nu})\}}.I(x) \tag{4.7}$$

This $I^{\dagger}(x)$ is truncated using an apodization function which in this case is a triangular. This step helps to reduce the side lobes from the deconvoluted Interferogram because sometimes it might be a problem when intensity of signal is same as that of a side lobe.

$$\begin{aligned} \mathbf{E}^{\dagger}(\bar{\nu}) &= \mathcal{F}\{A(x).I^{\dagger}(x)\} \\ &= \mathcal{F}\{A(x)\} * \mathcal{F}\{I^{\dagger}(x)\} \end{aligned} \tag{4.8}$$

where A(x) is the apodization function and is given by

$$A(x) = f(x)$$
$$= \begin{cases} 1 - \frac{|x|}{L}, \mid x \mid \leq L \\ 0, \mid x \mid > L \end{cases} \tag{4.9}$$

All the above operations were done in MATLAB and the function for triangular window function is 'triang(L)'where L is the size of the data that is to be truncated.

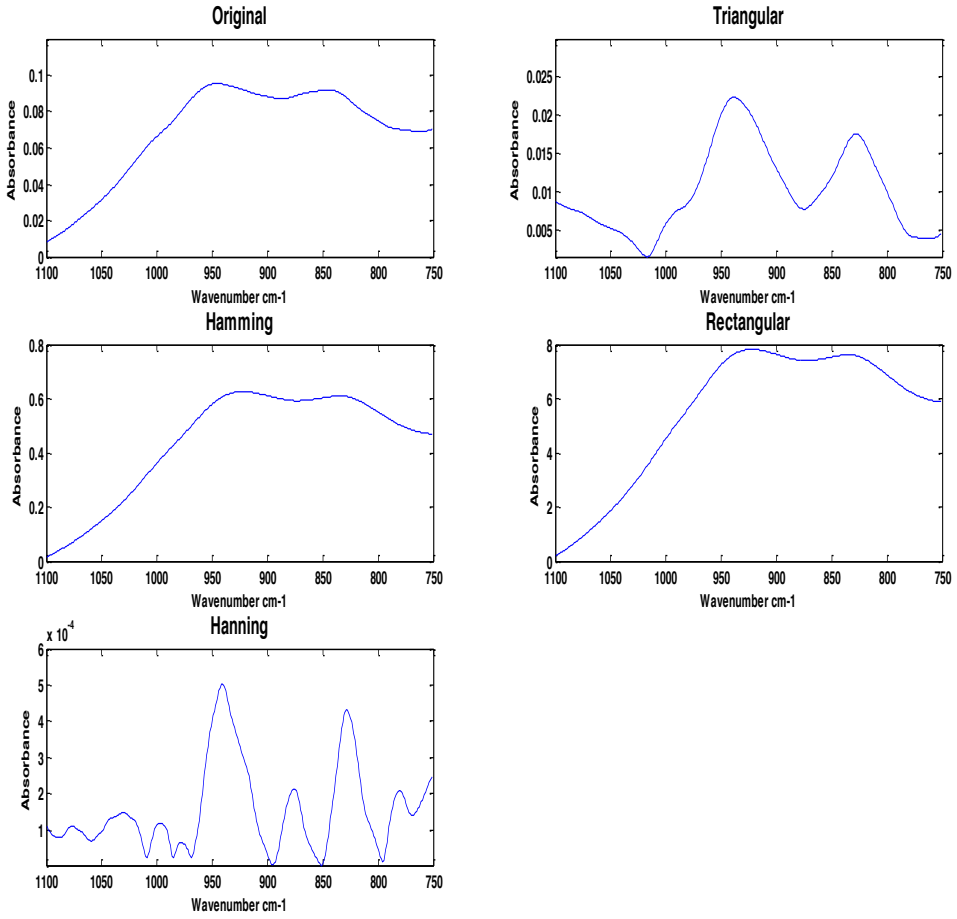

Figure 4.4: FTIR Deconvolution of Alkali Activated Slag Samples Using Different Window Functions.

The triangular window functions showed beneficial results for these samples avoiding over or under deconvolution. All the windowing functions are at different energy

levels. Hence for identification of peaks without concentrating on the actual absorbance values, these window functions can be used. As the triangular window function is a low energy filter, the absorbance values drop a little but the peak positions are not much altered.The obtained value $\mathbf{E}^{\dagger}(\bar{\nu})$ is the deconvoluted spectrum of $\mathbf{E}(\bar{\nu})$ Also, resolution enhancement factor K is considered as one of the input properties for the deconvolution procedure.

$$K(resolutionenhancementfactor) = \frac{HalfWidthoforiginalpeak}{Halfwidthofthelineshapefunction} \quad (4.10)$$

Here in our case, the ratio of half width at half maximum of $\mathbf{E}(\bar{\nu})$ to the HWHM of $\mathcal{S}(\bar{\nu})$ gives the value of K.

4.3 Curve Fitting

Many spectroscopists nowadays use the deconvolution and curve fitting techniques to get more intellect from the experimental spectra. Curve fitting techniques helps to separate the individual bands which are part of the integrated spectrum. The FTIR spectra obtained from the instrument or the deconvoluted spectra obtained from the program are both continuous integrated curves. But, to understand the contribution of the peaks present in the spectrum, the peaks are to be separated. The main parameters of the individual bands being HWHM (half width at half maximum) and the intensity can be obtained by the curve fitting process and this helps to compare the bands and their contribution to the parent spectra. To solve nonlinear least square problems, Levenberg-Marquardt is one of the standard techniques. The sum of squares of errors between function and the actual data points is minimized in the technique. This curve fitting method is actually a combination two different methods: Gradient descent method and Gauss-Newton Method. Based on the parameters it chooses to be more towards one of these two methods. The composites contain numer-

ous types of molecules which behave differently with their environment. Vibrational frequencies, shapes and modes depend on inter molecular interaction and also the interaction with the environment. The observed spectra or line shape of a particular sample is the combination or sum of all these different vibrating molecules. Fourier Self Deconvolution helps to discover or identify different contributions from different types of bonds in a single observed spectra band. But, the curve fitting technique helps to isolate these peaks as different individual bands from the spectrum. Fityk 0.9.8 is the software that has been used for the curve fitting analysis The Levenberg-Marquardt algorithm is used for the curve fitting analysis. The half widths at half maxima (HWHM) were obtained including the peak values (wavenumber). The R_2 values of all curve fits range from 0.96 to 0.99.

Figure 4.5: Illustration of The Fityk 0.9.8 Software Used For Curve Fitting of The De-Convoluted FTIR Data

Chapter 5

TIME AND TEMPERATURE DEPENDENT ANALYSIS OF ALKALI ACTIVATED SLAG

5.1 Effect of Curing Time

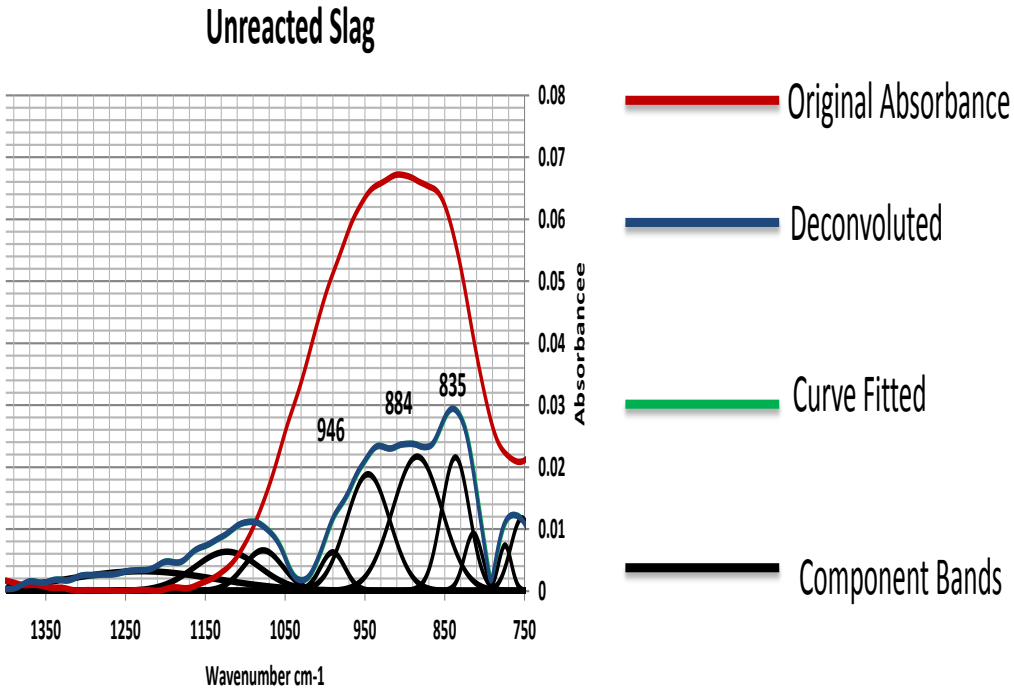

Figure 5.1: The Deconvoluted Peaks of Unreacted Slag Powder.

Figure 5.1 shows the deconvoluted peaks of unreacted slag powder using a Gaussian shape function and a resolution enhancement factor of 3.5 (approximately). The area of interest is 800 cm^{-1} to 1200 cm^{-1} as this range is indicative of the vibration modes that stem from the silica bonds. The peak at 946 cm^{-1} represents the asymmetric stretching vibration bond of Si-O-T where T can be Si or Al [36], [37], [38], [39], [40], [41], [42], [43]. The peak at 884 cm^{-1} represents the symmetric stretching

vibration of Si-O bond. The peak at 835 can be attributed to the Si-O asymmetric stretching band The peaks from 1020 to 1150 cm^{-1} can be attributed to the symmetric and asymmetric vibrations of unreacted silica present in the matrix. The asymmetric peak has two different wavenumber ranges which could be due to difference in their force constants values. Using these ranges as base values the peak values of alkali activated slag pastes were obtained and the variations in the curves over time were observed. The changes in the microstructure using FTIR deconvolution were observed over time. The alkali activated slag samples (activated both with 'Na 'and 'K 'Silicates) were tested at 6h, 12h, 1d, 2d, 7d, 14d, 28d.

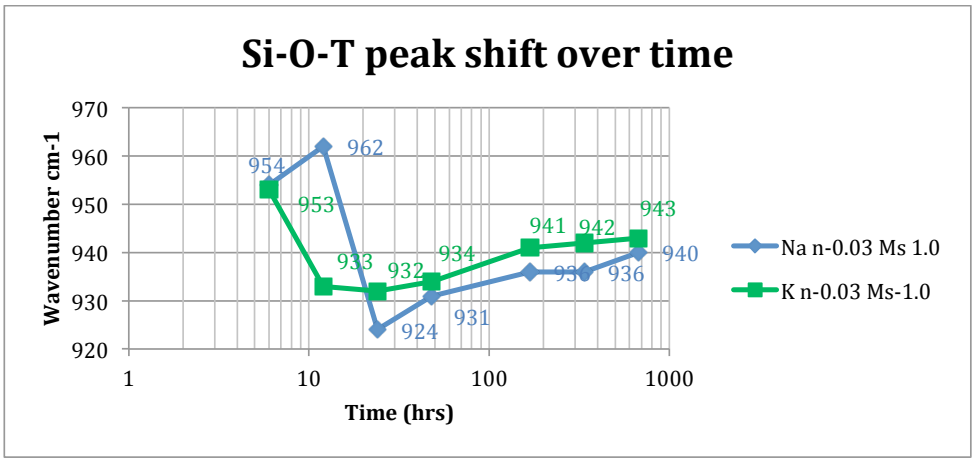

Figure 5.2: The Si-O-T Peak Shift of Slag Pastes Activated Using Na- silicate And K-silicate At 25°C from 6 hours to 28 days.

Figure 5.2 shows the change in wavenumber of Si-O-T peak over time for slag pastes activated with sodium and potassium Silicate using a 'n'value of 0.03 and 'Ms'of 1.0. The wavenumbers reach a higher value at the initial stages and drop to low numbers at about 20 hours from which there is a gradual increase in the wavenumbers with curing time. During the initial stages the symmetric peaks obtain high relative intensities which are due to the symmetric vibrations present in

the unreacted slag and added silicate species. Due to the incorporation of aluminum and the severing of silicate bonds, the symmetric bond vibrations develop asymmetric nature which increases the intensity of asymmetric vibrations in the structure. The absorbance in the FTIR spectra is in direct proportion with quantity thus, the intensity of asymmetric peak increases with more Al incorporation in to the system. From figure 5.1 for sodium silicate activated slag we can observe that there is an increase in the wavenumber till 12 hours of activation and drops to lower wavenumber of 924 cm^{-1} after 1 day. But the potassium activated slag shows a drop at 12 hours of activation without an increase in the wavenumber. Due to the higher polarizing effect of Na ion, it is capable to break the silicate bonds to incorporate aluminum at early ages which increase the wavenumber initially due to better polymerization. Potassium ion is capable to keep the soluble silica stable for a longer duration as compared to sodium ion [44], [45]. This could be the reason that there is no increase in the wavenumber of Si-O-T peak for potassium silicate activated slag pastes at the initial stages. The initial high wavenumbers appear due to the existence of peaks at 810-820 cm^{-1} and 895-905 cm^{-1} due to the symmetric and asymmetric bond vibrations at the initial stages. Due to their contribution to the integrated curve the main Si-O-T peak is pushed to a higher wavenumber due to similarities in the relative intensities. With curing time and more of Al incorporation and the intensity of Si-O-T peak being dominant, the wavenumbers fall back indicating that the increase in the amount of Si-O-T bond vibrations resulting in a higher networked or denser structure. The NMR studies of alkali activated slag pastes show that the amount of Q2 structure is high in the system after 28 days of activation which can be attributed to the dominant relative intensities of Si-O-T bonds in the matrix.

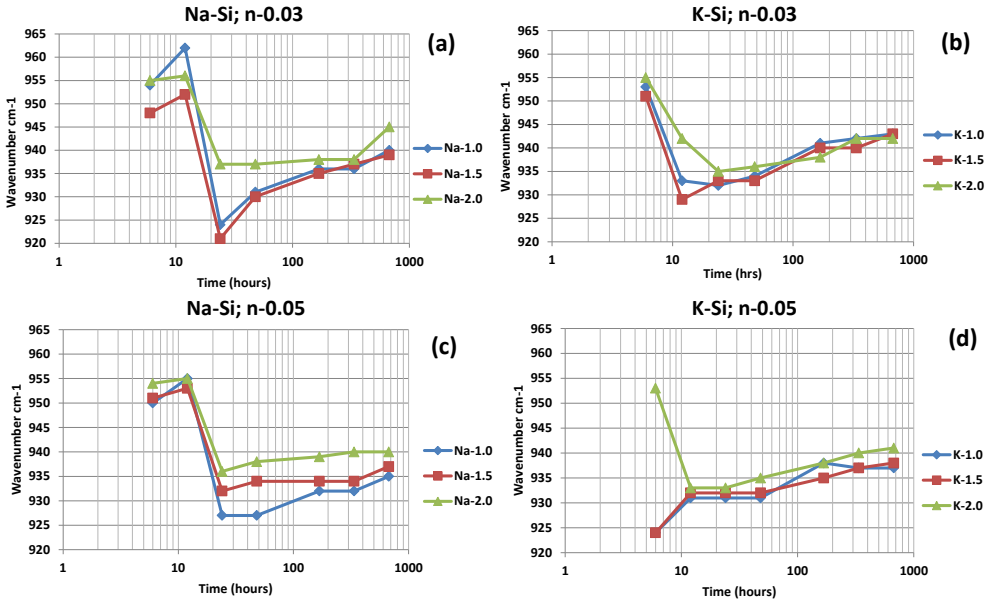

Figure 5.3: Si-O-T Peak Shifts of Activated Slag Pastes(a) Na-Si Activator With 'n'of 0.03, (b) K-Si Activator With n of 0.03, (c) Na-Si Activator With 'n'of 0.05, (d) K-Si Activator with 'n'of 0.05.

5.1.1 Influence of Alkalinity ('n'and 'M_s')

Figures 5.3 (a), (b), (c), (d) shows the change in wavenumber of Si-O-T peak over time for slag pastes activated with sodium and potassium silicates with 'n'values of 0.03, 0.05 and 'M_s'values of 1.0, 1.5, 2.0. The desired 'n'value is attained and hydroxides are added to attain different Ms values. From Figure 5.3 we can compare the trends that were observed in Figure 5.3. Except for the mixes with potassium silicate activator with 'n'of 0.05 and 'M_s'values of 1.0 and 2.0 all the other mixes show similar trends as in the observations from Figure 3. The mixes with potassium silicate activator and with 'n'of 0.05 have higher amount of hydroxides and silicates in the system comparatively which show earlier drop in the Si-O-T peak. But when 'M_s'is 2.0 the silicate content is comparatively higher and due to less polarizing nature of

potassium the soluble silicates will be kept stable for a longer duration comparatively.

From Figures 5.3 (a), (b), (c), (d) we can observe that the mixes with 'n'of 0.03 reach higher wavenumbers at 28 days compared to the mixes with 'n'of 0.05. Due to higher concentration of hydroxides than silicates (comparatively) the numbers of silicate bonds in the system are relatively lower which increases the possibility for severing and incorporating more aluminum in to the system which ultimately show better polymerization that is depicted from the higher wavenumber values. In the case with n of 0.05 the presence of more amounts of silicates may allow the hydroxides to break the silicate bonds even after 28 days. This can be related to the lower wavenumber values observed from the mixes with 'n'of 0.05. We can observe that in all the mixes the ones with M_s of 2.0 attain relatively higher wavenumbers compared to ones with 'M_s'of 1.0 and 1.5. Due to the higher amounts of silicates comparatively, more bonds can be severed to incorporate more aluminum in to the structure resulting a structure with relatively higher polymerization. Although the values are relatively close in every plot, the trends can still be comparable.

The sharpness of a peak can be related to its Half Width at Half Maximum (HWHM). As increase in wavenumber can be attributed to attaining better degree of polymerization similarly increase in the sharpness of a peak can also be attributed to the presence of one species of silica bond in abundance thus it can be related to the uniqueness of a particular vibration depicted from that peak. The results from Figure 5.4 (a), (b), (c), (d) can be correlated to the plots from Figure 5.3 (a), (b), (c), (d). Even though the values are approximately following a similar trend, the curves depict the increase in the polymerization degree of alkali activated slag pastes over time due to a gradual decrease in the HWHMs of the Si-O-T peaks. For the sodium silicate activated slag pastes from figure 5.4(a), (c) there is a decrease in the HWHM initially which can be correlated to increase in Si-O-T peak wavenumber from figures

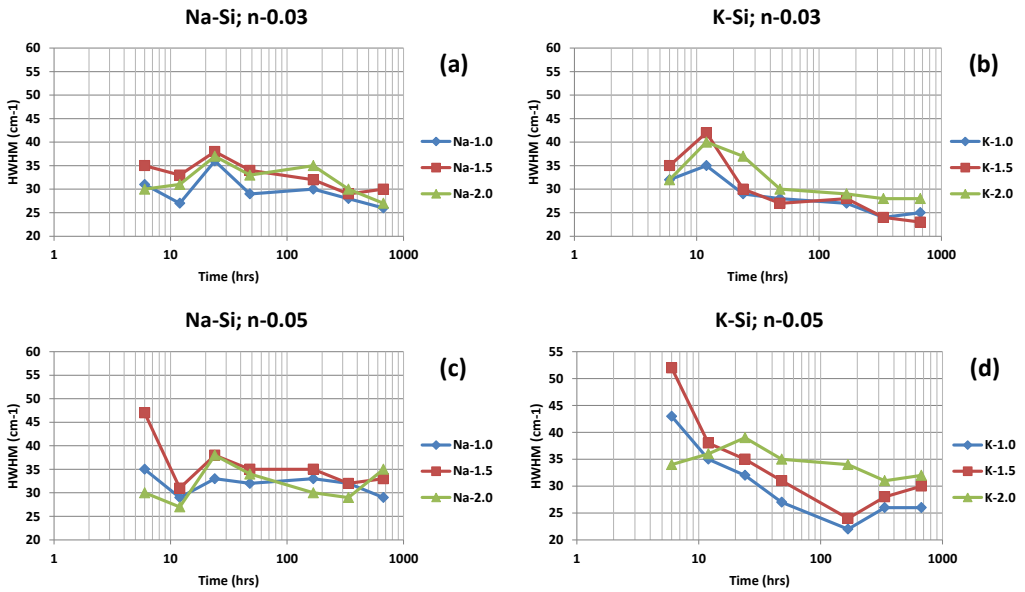

Figure 5.4: HWHM Of Si-O-T Peak For Alkali Activated Slag Pastes, (a) Na-Si Activator With 'n'of 0.03, (b) K-Si Activator With 'n'of 0.03, (c) Na-Si Activator With n of 0.05, (d) K-Si Activator Activated With n of 0.05.

5.4 (a), 4(c). Similarly the slag pastes activated with potassium silicates from figures 5.4 (b), (d) the trends are different for mixes with 'n'of 0.05 and 'M_s'values of 1.0 and 1.5 which again can be correlated to gradual increase in Si-O-T peak wavenumbers without any drop observed in figures 5.4 (b), (d).

5.1.2 Influence of Cation (Na and K)

The alkaline nature created in the slag pastes after activation is due to the presence of sodium and potassium ions from the activators. This enhances the ability to incorporate aluminum in to the gel structure by breaking the silicate bonds. Presence of these ions can also be seen in the polymerized chains of silica.

From all the previous plots we observed significant differences between the deconvoluted FTIR plots of sodium silicate and potassium silicate activated slag pastes. Comparing the results from Figures 5.3(a), 5.3(b) with results from Figure 5.3(c),

5.3(d) we can observe that the sodium silicate activated pastes have much variation in the trends with change in M_s than the potassium silicate activated pastes. As sodium has a better polarizing nature, it is capable to sever the silicate bonds present in the system in better nature ultimately incorporating more aluminum in to the structure. This is because the hydration sphere of sodium ion is larger compared to the potassium ion. Also, initially Sodium silicate activated slag pastes show earlier increase in the Si-O-T peak shifts which is not seen in the potassium silicate activated pastes. Potassium is capable to keep the soluble silica stable for longer durations compared to sodium which can prevent the initial breakage of silicate bonds in to the system.

5.2 Effect of Temperature

5.2.1 Influence of Alkalinity ('n'and 'M_s')

To encounter the changes in the reaction mechanism, the samples have been heat cured at two different temperatures 80°C and 60°C in an oven. The FTIR spectra have been obtained at different time steps up to a period of three days. The times at which the spectra have been extracted are 3h, 6h, 12h, 1day, 2day and 3days. Activators used were Sodium Silicate and Potassium Silicate with 'n'vales of 0.03 and 0.05 and M_s of 1.5. Figures 5.5(a), (b) show the Si-O-T peak shift of slag pastes activated with Sodium and Potassium silicates which were cured at 60° C. Figures 5.5(c), (d) show the Si-O-T peak shift of slag pastes activated with Sodium and Potassium silicates which were cured at 80° C.

In contrast to the results obtained from samples cured at 25°C the heat cured samples show much earlier polymerization which can be attributed due to activation energy obtained from the heat to polymerize faster. From figures 5.5(a),(b) we can

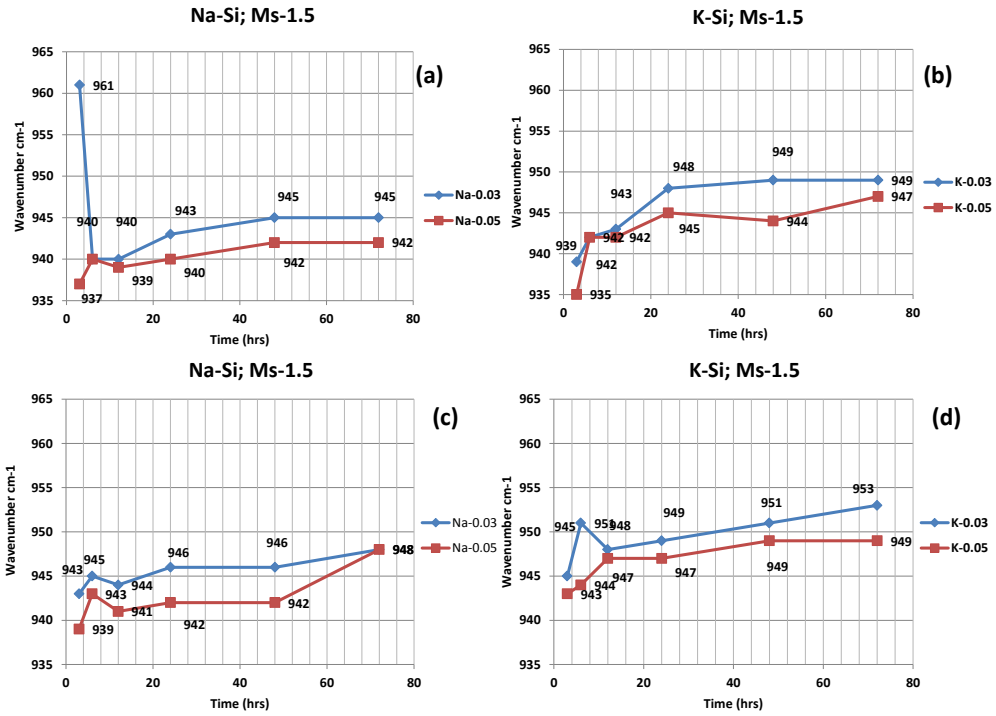

Figure 5.5: Alkali Activated Slag Cured At High Temperatures Showing Si-O-T Peak Shift With Time (a) Na-Si Activator at 60°C, (b) K-Si Activator at 60°C, (c) Na-Si Activator at 80°C, (d) K-Si Activator at 80°C.

observe that all the activated slag samples cured at 60° C reach a lower wavenumber before 3 hours of activation except for the case with Sodium silicate activated slag with 'n'of 0.03. This could be due to the fewer amounts of silicates and hydroxides from the activator which takes time to form a dense polymerized network. Eventually with increase in curing time the samples with lower 'n'value show increased polymerization which can be depicted from the wavenumber values. The samples with higher 'n'value (0.05) have higher amounts of silica and hydroxides available in the system. The silicate bonds are available to be broken even after a period of 72 hours. The severing causes the discontinuity in the polymerization chains, this makes the samples to attain a lower wavenumber compared to the samples with 'n'of 0.03.

The samples cured at 80° C from figure 5.5(c),(d) attain the lower wavenumbers before 3 hours of curing time. Due to the enhancement of the kinetics in the system the polymerization happens at a faster rate compared to curing at 25° C and 60° C. An initial peak after 6 hours could be due to formation of products at the early ages. Similarly to the trends from figures 5.5(a), (b) the samples cured at 80° C also show that the ones with lesser n values obtain higher wavenumbers. The samples cured at 80° C (from Figures 5.5(c), (d)) show higher wavenumber values than the ones cured at 60° C (from Figures 5.5(a), (b)) due to higher amount of heat supplied to increase the reaction kinetics forming higher polymerized products.

5.2.2 Influence of Cation (Na and K)

The heat cured samples show better early age reaction products due to the provision of energy to enhance the process. When comparing the Si-O-T peaks shift plots between the sodium silicate and potassium silicate activated pastes from Figures 5.5 (a), (b), (c), (d); we can observe that potassium silicate activated slag samples attained higher wavenumbers consistently at every time step compared to sodium silicate activated slag pastes. The heat supplied to the system increase the kinetics and also the mobility of ionic particles in the matrix. Though potassium ion has less polarizing effect than sodium, the smaller ionic radius of potassium ion and the supplied heat make it more mobile compared to sodium ion. This can lead the potassium silicate activated pastes to form better polymerized products.

5.3 Effect of Silica Polymerization On Strength

5.3.1 Correlation of Compressive Strength

Figure 5.6 shows the compressive strength development of Sodium and Potassium Silicate Activated Slag pastes with 'n'value of 0.05 and 'M_s'of 1.5. The results obtained are at 1day, 7day and 28 days. The Figure shows that with an increase in the wavenumber of the Si-O-T peak the strengths are developing. The wavenumber increase which can be attributed to the development in the polymerization of the structure which in a way densifies the matrix gives better compressive strengths to the samples. This correlation describes the relation between the increase in the wavenumber of the Si-O-T peak with time and the strength developed over time where the conclusion can be made for all the other mixes used for the FTIR deconvolution analysis.

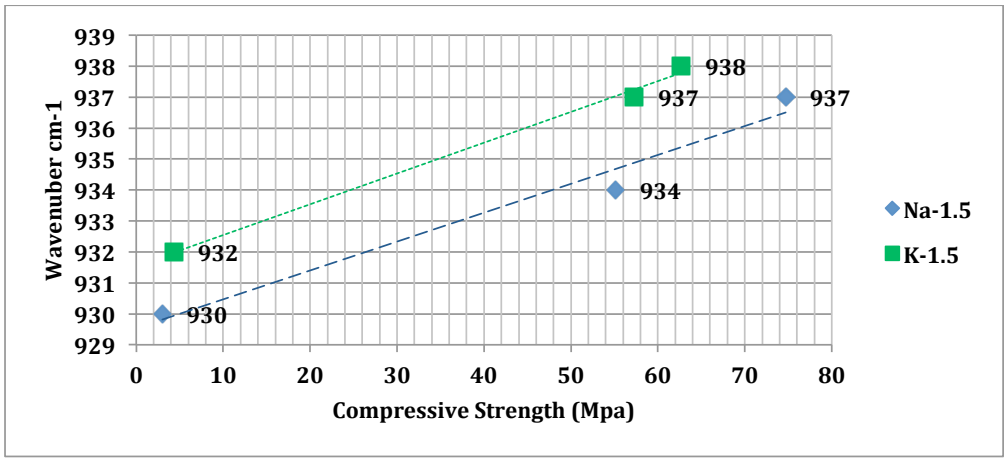

Figure 5.6: Compressive Strength Development of Sodium And Potassium Silicate Activated Slag Pastes.

Chapter 6

FTIR ANALYSIS OF ALKALI ACTIVATED FLY ASH

Fly Ash does not set quickly on alkali activation unlike slag. The samples are to be heated at high temperatures for the material to initiate the reaction process. The fly ash samples have been activated by alkali medium with and without silicate solutions. Studies showed that the presence of soluble silicates in the activating solutions show significant change in the product formation as compared to activators without soluble silicates. The soluble silicates accelerate the dissolution process in fly ash [6]. But in our study all the samples are analyzed under same curing conditions i.e. cured at 80° C for 72 hours. The variations in the products can be observed by determining their peak positions and the properties of peaks (half width at half maximum). Studies have shown that the alkali silicate activated samples show better polymerization than the ones activated with alkali hydroxides. The presence of silicate monomers in the activator provides more polymerization chains with silicate content. Whereas, the hydroxide activators lead to dissolution of fly ash and the formed gel is rich in polymers with more aluminum present in the chains. The presence of more Si-O-Al bonds decreases the wavenumber of Si-O-T peak which indicates lower degree of polymerization.

6.1 Alkali Hydroxide Activated Systems- Effect of Concentration

Aluminosilicate materials like fly ash undergo a dissolution process in an alkaline environment to further repolymerizes to form solid products that show properties similar to traditional cements. Class-F fly ash has been activated with alkali hydroxides at different concentrations and the reaction products are tested using FTIR

spectrometry. Sodium and Potassium hydroxides were used at 3 different molar ratios and the properties of the resultant Si-O-T peaks were observed to analyze the reaction products which were cured at 80° C for 72 hours in a sealed environment. An aluminum rich gel forms initially before the final gel composition is attained. The polymerization of silicate chains happens later on after these initial products are formed. From figure 6.1 we can observe that for samples activated with NaOH

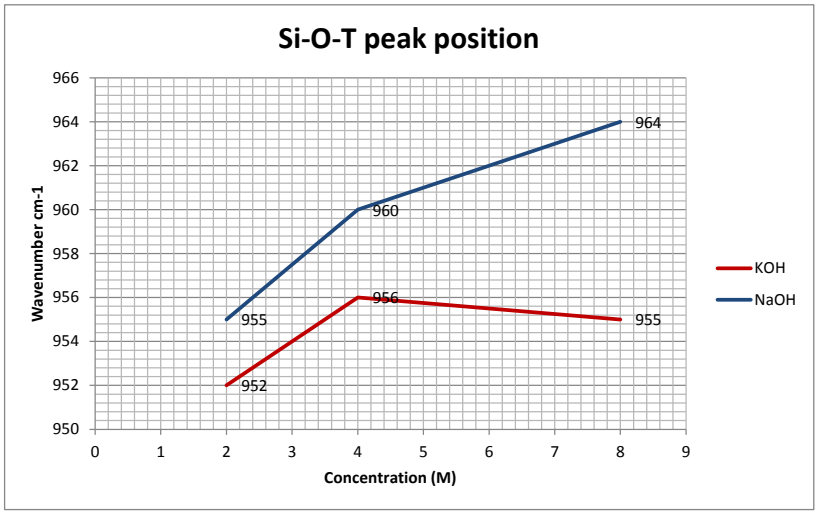

Figure 6.1: Si-O-T Peak Position Of NaOH and KOH Activated Fly Ash With Variation In Concentration.

activator the position of peak is shifting to a higher wavenumber with increase in concentration. As the concentration increases, the alkalinity increases in the system with lead to increased dissolution of fly ash. Activators with higher concentration incorporate more aluminum in to the structure to form a better polymerized product. But the samples activated with KOH activators do not show much change in the Si-O-T peak position with increase in the concentration. The polarization nature of Na^+ ion is greater than K^+ ion and also size of hydration sphere of potassium ion is smaller compared to that of sodium ion. Hence, the ability to severe the silica bonds in the structure and incorporate aluminum is lesser for potassium hydroxide activators. From the figure 6.1 we can observe that not much change in the position of the Si-O-T

peak from 4M concentration to 8M concentration activator but for NaOH activated samples significant change has been observed with increase in the concentration of the activator. The half width at half maximum (HWHM) indicates the sharpness of

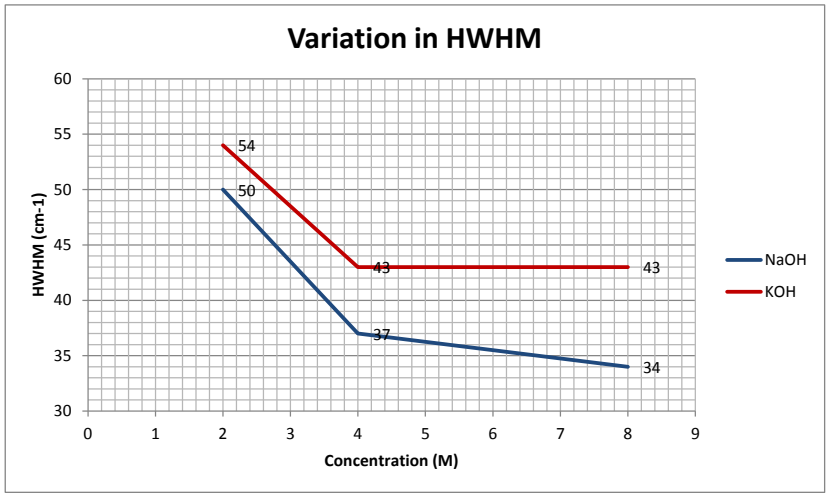

Figure 6.2: Variation Of HWHM Of Si-O-T Peak of Both NaOH And KOH Activated Fly Ash W.R.T Concentration Of The Activators.

the peak. The sharpness of a peak signifies the uniqueness of a particular vibration contributing to that peak. From figure 6.2 we can observe that the trend goes similar to that of the plot showing the variation in the position of Si-O-T peak in figure 6.1. In the potassium hydroxide activated samples, there is no change in the half width when the concentration is increased from 4M to 8M. Whereas in the NaOH activated samples, significant change can be observed in the HWHM with increase in concentration. The ability of sodium ion to sever the bonds to incorporate aluminum in to the structure is greater than potassium. Form figure 6.1 we can see that the NaOH activated samples possess greater wavenumbers than KOH activated samples which indicate better polymerized products as the binding matrix i.e. fly ash is same for all the samples. Similarly, in figure 6.2 the half width values of NaOH activated samples are lesser then KOH activated samples correlating the results from figure 6.1. The variation in the wavenumbers is not so high with change in the concentration of the

activator. Studies have shown that the presence of added silicates in the activators increase the dissolution of fly ash and form better polymerized products than the products formed due to activators with just hydroxides in them [6].

6.2 Alkali Silicate Activated Systems

The effect of alkali activation on fly ash has been observed using alkali hydroxides as activators. Silicates have been added to the activators with different R/Al ratios (where R is Na or K) and M_s (silica modulus). The soluble silicates added through the activators do play an active role in forming the reaction products. The silicate monomers present in the matrix polymerize with the chains in the matrix to form a better polymerized product. The variation in the Si-O-T peak with different R/Al ratios and M_s has been observed and compared with the variations observed in the hydroxide activated sample results. The consistent increase in the wavenum-

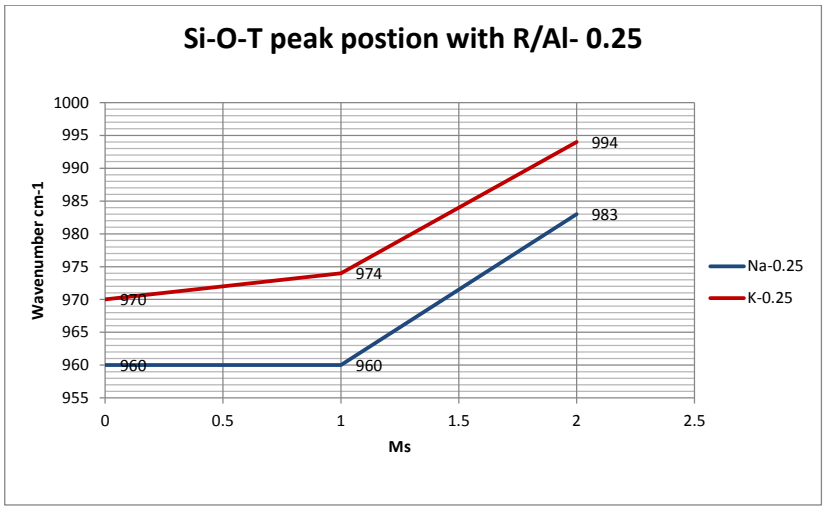

Figure 6.3: The Si-O-T Peak Position For R/Al Ratio Of 0.25 With Variation In M_s.

ber with increase in M_s can be observed from figure 6.3. The peak position values are much higher than the values observed in figure 6.1 for fly ash samples activated with only hydroxides. The presence of soluble silicates in the system allows better

polymerization of the structure as the number of Si-O-T vibrations increase in the matrix providing a better degree of polymerization. Increase in M_s at a fixed R/Al ratio indicates increase in the amount of added soluble silicates. This leads the system to form better polymerized products as the soluble silicates added to the system polymerize together with the silicate chains.

The samples activated with potassium silicate activators obtain higher wavenumbers consistently when compared to sodium silicate activated systems. Similar results have been observed in chapter 5 where the slag samples are heat cured for 3 days. Potassium ion is capable to keep the soluble silica stable for a longer duration than sodium ion. Also, the smaller size of potassium ion can be more mobile compared to the sodium ion. The heat provided to these systems increase the reaction kinetics and this energy creates movement of ions in the system. Potassium ion being more mobile can react at a higher rate due to the provision of heat in to the system. Also, the added silicates enhance the reaction of the system and form better polymerized products than in the case where alkali hydroxides are used as activators. Similar

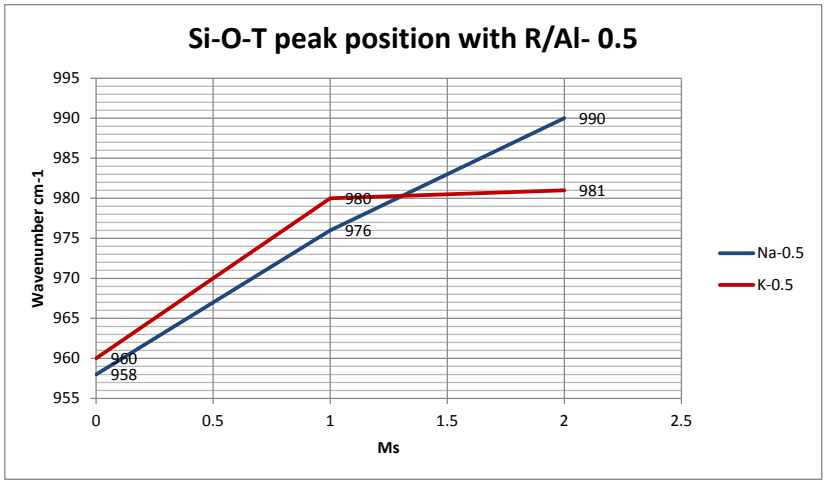

Figure 6.4: The Si-O-T Peak Position For R/Al Ratio Of 0.5 With Variation In M_s.

trend can be seen from figure 6.4 as in the results shown in figure 6.3. The gradual increase in wavenumber with increase in the wavenumber explains the role of added

silicates in to the system. But in this case both the silicates and alkali ion will be in higher amount compared to an R/Al ratio of 0.25. Here the wavenumbers are in a comparable difference between sodium silicate activated and potassium silicate activated systems but still the ranges are higher than the system activated with hydroxides. From the figure 6.4 we can see that except for the case with M_s of 2.0, potassium silicate activated samples show higher wavenumber than sodium silicate activated sample. The marginal difference between sodium and potassium silicate activators is higher in the case with R/Al ratio of 0.25. Due to the presence of lower number of ions (alkali) and added silicates, the effect of added silicates dominates the effect of cation. As potassium ion is capable to keep the soluble silica stable for longer duration and due to the high mobility, the potassium silicate samples show a significant and consistently higher wavenumbers compared to sodium silicate activated samples. Whereas in the case with R/Al ratio of 0.5, the alkaline effects of the cation is comparably similar due to the higher alkalinity. Hence the results were comparatively similar. But in both the cases where added silicates are present in the activators, better polymerized products were observer than hydroxide activated fly ash samples. Also, with increase in the M_s the position of Si-O-T peak shifts to a higher wavenumber by attaining better degree of polymerization.

Chapter 7

CONCLUSIONS

The aim of this research is to understand the changes in polymerization of alkali activated slag and fly ash pastes concentrating on the effects of time, effects of temperature, influence of mix proportion parameters and the influence of cation type on the polymerization. The parameters in the Fourier self deconvolution algorithm were kept consistent to reduce the effects of the parameters on the obtained results. Although the triangular window used is a low energy filter, it showed best results for qualitative analysis compared to the other traditional window functions. The Si-O-T asymmetric peak was concentrated as the structural changes in the reaction products for alkali activated slag pastes were best explained from the deconvoluted peaks.

7.1 Time and Temperature Dependent Analysis of Alkali Activated Slag

1. The samples with lower n values show better polymerized products which were attributed from higher wavenumber values since the amount of silicates and hydroxides are higher in the samples with higher n values which result in further severing of silicate bonds decreasing the degree of polymerization of the products.
2. The samples with higher M_s in the same n value show better polymerization due to the availability of more silicates in the system for breakage and incorporation of aluminum. Although the later age wavenumbers are in a comparable range for both Sodium and Potassium silicate activated slag pastes, significant changes can be observed at early ages where Sodium silicate activated samples show a development in the wavenumber due to the high polarizing nature.

3. The heat cured samples show earlier polymerized results due to the heat supplied to the samples which enhances the kinetics of the system making the molecules to react at a faster rate. Similar to the samples cured at room temperature, the heat cured samples also depict better polymerization for mixes with lower n value.
4. The Potassium silicate activated samples attain higher wavenumbers due to increase in the Brownian motion of the ions. The lesser ionic size of potassium ion makes it more mobile leading to form better reaction products than sodium silicate activated samples.

7.2 FTIR Analysis of Alkali Activated Fly Ash

1. The effect of cation (Na and K) is different for fly ash activated with alkali hydroxides and fly ash activated with alkali silicates. The capability of potassium to keep the soluble silica stable cannot be observed in the absence of soluble silica from the activator. As the polarizing nature of sodium ion is higher the polymerization is enhanced when fly ash is activated with only hydroxides without silicates.
2. The degree of polymerization attained is better when there are silicates in the activators. The presence of added silicates increase the polymerization in the matrix as more and more silicate monomers can be attached to the chains and also aluminum incorporation occurs due to the alkaline environment.

The Si-O-T peak values are higher in fly ash compared to slag. The silica and alumina content in fly ash are higher compared to slag. More polymerized chains can be present as the quantity is higher. This leads to the structures to attain higher polymerization degrees.

REFERENCES

[1] Huajun Zhu, Zuhua Zhang, Yingcan Zhu, and Liang Tian. Durability of alkali-activated fly ash concrete: Chloride penetration in pastes and mortars. *Construction and Building Materials*, 65(0):51 – 59, 2014.

[2] SA. Bernal, R. Mejia de Gutierrez, and R. Provis JLPabst. Engineering and durability properties of concretes based on alkali-activated granulated blast furnace slag/metakaolin blends. *Construction and Building Materials*, pages 99–108, 2012.

[3] J. Bijen. Benefits of slag and fly ash. *Construction and Building Materials*, 10:309–14, 1996.

[4] J. Grdadolnik. Atr-ftir spectroscopy: Its advantage and limitations. *Acta Chim Slov*, 49:639–42, 2002.

[5] GC. Lukey and JSJ. van Deventer. In situ atr-ftir study of the early stages of fly ash geopolymer gel formation. *Langmuir*, 23:9076–82, 2007.

[6] CA. Rees, JL. Provis, GC. Lukey, and JSJ. van Deventer. Attenuated total reflectance fourier transform infrared analysis of fly ash geopolymer gel aging. *Langmuir*, 23:8170–9, 2007.

[7] VD. Glukhovsky, GS. Rostovskaja, and GV. Rumyna. High strength slag-alkaline cements. *Proc. 7th Int. Congr. Chem. Cem. Paris.*, 1980.

[8] J. Davidovits. Geopolymers and geopolymeric materials. *Therm Anal*, 35:429–41, 1989.

[9] P. Duxson, A. Fernndez-Jimenez, JL. Provis, GC. Lukey, Palomo A, and JSJ van Deventer. Geopolymer technology: the current state of the art. *Mater Sci*, 42:2917 33, 2007.

[10] P. Duxson, JL. Provis, GC. Lukey, and JSJ van Deventer. The role of inorganic polymer technology in the development of green concrete. *Cem Concr Res*, 37:1590 7, 2007.

[11] N. Mahasenan, S. Smith, K. Humphreys, and Y. Kaya. The cement industry and global climate change: current and potential future cement industry co2 emissions. greenh. *Gas Control Technol. 6th Int. Conf. Oxf. Pergamon*, page 995 1000, 2003.

[12] Palomo A. Alonso, and. Alkaline activation of metakaolin and calcium hydroxide mixtures: influence of temperature, activator concentration and solids ratio. *Mater Lett*, 47:55 62, 2001.

[13] D. Khale and R. Chaudhary. Mechanism of geopolymerization and factors influencing its developmen, a review. *Mater Sci*, 42:729 46, 2007.

[14] D. Hardjito, DM. Sumajouw, S. Wallah, and Bv. Rangan. Fly ash-based geopolymer concrete. *Aust J Struct Eng*, 6:77, 2005.

[15] R. Ylmen, U. Jaglid, B-M. Steenari, and I. Panas. Early hydration and setting of portland cement monitored by ir, sem and vicat techniques. *Cem Concr Res*, 39:433 9, 2009.

[16] S-D. Wang and KL. Scrivener. Hydration products of alkali activated slag cement. *Cem Concr Res*, 25:561 71, 1995.

[17] S. Astutiningsih and Y. Liu. Geopolymerisation of australian slag with effective dissolution by the alkali. *World Congr. Geopolymer, Saint Quentin, France*, 25:6973, 2005.

[18] D. Dimas, I. Giannopoulou, and Panias D. Polymerization in sodium silicate solutions: a fundamental process in geopolymerization technology. *J Mater Sci*, 44:3719–30, 2009.

[19] Chithiraputhiran SR.. Kinetics of alkaline activation of slag and fly ash-slag systems. 2012.

[20] MB. Haha, B. Lothenbach, G. Le Saout, and F. Winnefeld. Influence of slag chemistry on the hydration of alkali-activated blast-furnace slagpart i: Effect of mgo. *Cem Concr Res*, 41:955–63, 2011.

[21] Hajimohammadi A., Provis JL., and van Deventer JS. The effect of silica availability on the mechanism of geopolymerisation. *Cem Concr Res*, 41:210–6, 2011.

[22] D. Hardjito, Bv. Rangan, and et al. Development and properties of low-calcium fly ash-based geopolymer concrete. *Perth Aust Curtin Univ Technol*, 41:210–6, 2005.

[23] C09 Committee. Specification for slag cement for use in concrete and mortars. *ASTM International*, 2013.

[24] Yip Ck., Lukey GC., and van Deventer JSJ. he coexistence of geopolymeric gel and calcium silicate hydrate at the early stage of alkaline activation. *Cem Concr Res*, 35:1688–97, 2005.

[25] Chithiraputhiran S. and Neithalath N. Isothermal reaction kinetics and temperature dependence of alkali activation of slag, fly ash and their blends. *Constr Build Mater*, 45:23342., 2013.

[26] M Ben Haha, G Le Saout, F Winnefeld, and B Lothenbach. Influence of activator type on hydration kinetics, hydrate assemblage and microstructural development of alkali activated blast-furnace slags. *Cem Concr Res*, 41:30110, 2011.

[27] A Fernandez Jimenez, F Puertas, I Sobrados, and J Sanz. Structure of calcium silicate hydrates formed in alkaline-activated slag: influence of the type of alkaline activator. *J Am Ceram Soc*, 86:138994, 2003.

[28] A Fernandez Jimenez and F Puertas. Setting of alkali-activated slag cement. influence of activator nature. *Adv Cem Res*, 13:11521, 2001.

[29] D Ravikumar and N Neithalath. Effects of activator characteristics on the reaction product formation in slag binders activated using alkali silicate powder and naoh. *Cem Concr Compos*, 34:80918, 2013.

[30] T Bakharev, JG Sanjayan, and Y-B Cheng. Effect of elevated temperature curing on properties of alkali-activated slag concrete. *Cem Concr Res*, 29:161925, 1999.

[31] JK Kauppinen, DJ Moffatt, HH Mantsch, and DG. Cameron. Fourier self- deconvolution: A method for resolving intrinsically overlapped bands. *Applied Spectroscopy*, 35:2716, 1981.

[32] JK Kauppinen, DJ Moffatt, HH Mantsch, and DG. Cameron. Fourier transforms in the computation of self-deconvoluted and first-order derivative spectra of overlapped band contours. *Anal Chem*, 53:1454–7, 1981.

[33] Tooke PB. Fourier self-deconvolution in ir spectroscopy. *TrAC Trends Anal Chem*, 7:130–6, 1988.

[34] Andreev GN. Kochev NT, Rogojerov MI. A new graphical approach for improved user control of fourier self-deconvolution of infrared spectra. *Vib Spectrosc*, 25:177–83, 2001.

[35] JK Kauppinen, DJ Moffatt, HH Mantsch, and DG. Cameron. Noise in fourier self deconvolution. *Appl Opt*, 20:1866, 1981.

[36] M. Wojdyr. Fityk : a general-purpose peak fitting program. *J Appl Crystallogr*, 43:1126–8, 2010.

[37] P Rovnank, P Bayer, and P. Rovnankova. Characterization of alkali activated slag paste after exposure to high temperatures. *Constr Build Mater*, 47:1479–87, 2013.

[38] I Garca Lodeiro, DE Macphee, A Palomo, and A. Fernandez-Jimnez. Effect of alkalis on fresh csh gels. ftir analysis. *Cem COnc Res*, 39:147–53, 2009.

[39] I Garca-Lodeiro, A Fernandez-Jimenez, MT Blanco, and A. Palomo. Ftir study of the solgel synthesis of cementitious gels: Csh and nash. *J Sol-Gel Sci Technol*, 45:63–72, 2008.

[40] F Puertas and A. Fernandez-Jimenez. Mineralogical and microstructural characterisation of alkali-activated fly ash/slag pastes. *Cem Concr Compos*, 25:287–92, 2003.

[41] F Puertas, A Fernandez-Jimenez, and MT. Blanco-Varela. Pore solution in alkaliactivated slag cement pastes. relation to the composition and structure of calcium silicate hydrate. *Cem Concr Res*, 34:129–48, 2004.

[42] W Mozgawa and J. Deja. Spectroscopic studies of alkaline activated slag geopolymers. *J Mol Struct*, 924-926:434–41, 2009.

[43] WKW Lee and JSJ. van Deventer. Use of infrared spectroscopy to study geopolymerization of heterogeneous amorphous aluminosilicates. *Langmuir*, 19:872634, 2003.

[44] Marzke R Neithalath N. Dakhane A, Peng Z. The effects of cationic type (na, k) on reaction kinetics and products of alkali activated slag n.d.

[45] A Fernandez-Jimenez, A Palomo, and M. Criado. Alkali activated fly ash binders. a comparative study between sodium and potassium activators. *Mater Constr*, 56:51–65, 2006.